Available online at www.sciencedirect.com
ScienceDirect
Ceramics International 35 (2009) 2351–2355
CERAMICS INTERNATIONAL
www.elsevier.com/locate/ceramint

Dielectric properties and phase transition in $SrBi_2Nb_2O_9$–$SrBi_2Ta_2O_9$ solid solution

D. Kajewski [a,*], Z. Ujma [a], K. Szot [a,b], M. Pawełczyk [a]

[a] *Institute of Physics, University of Silesia, 40-007 Katowice, ul. Uniwersytecka 4, Poland*
[b] *Institut für Festkörperforschung, Forschungszentrum Jülich, 52425 Jülich, Germany*

Received 21 July 2008; received in revised form 4 December 2008; accepted 22 January 2009
Available online 11 February 2009

Abstract

Structural and dielectric properties of $SrBi_2(Nb_{1-x}Ta_x)_2O_9$ solid solution, (SBNT), with $x = 0.0$, 0.1, 0.2, 0.3, 0.5, 0.7, 1.0 were investigated. Crystal structure at room temperature was analyzed by X-ray diffraction study. SBNT exhibits an Aurivillius structure and the c lattice constant decreases with increasing concentration of Ta in the solution. The studies of real (ε') and imaginary (ε'') parts of permittivity as a function of temperature (20–500 °C) and frequency (0.1–100 kHz) were carried out, as well. The anomalies of $\varepsilon'(T)$ and $\varepsilon''(T)$ associated with phase transition from the tetragonal paraelectric phase (P_T) to the orthorhombic ferroelectric phase (F_O) were observed. They are strongly dependent on the Ta content in the solution. The grain structure and chemical composition were examined by a scanning electron microscope (SEM), with an energy dispersion spectrometer (EDS). The EDS analysis indicated a homogeneous distribution of all elements of ceramics within the grains.

Keywords: B. Electron microscopy; B. X-ray methods; C. Dielectric properties; D. Perovskites

1. Introduction

An increasing interest in bismuth layer structured ferroelectrics (BLSFs) has been noticed in the recent years because of their potential application in technical devices. For example, Sr-based BLSFs such as $SrBi_2Nb_2O_9$ (SBN), $SrBi_2Ta_2O_9$ (SBT) and their solid solutions $SrBi_2(Nb_{1-x}Ta_x)_2O_9$ (SBNT) have been considered as one of the most promising candidates for non-volatile random access memory (NVRAM) devices due to their excellent fatigue-resistant properties [1]. The layer structure BLSFs, that is described by the chemical formula: $(Bi_2O_2)^{2+}$ $(A_{m-1}B_mO_{3m+1})^{2-}$, where m indicates the number of perovskite building blocks between two $(Bi_2O_2)^{2+}$ layers and A and B represent the different cations of low and high valences, allows to assume that there exists a great possibility for a mutual doping within various ions to BLSFs [2].

A lot of attempts to improve properties of the SBNT materials by doping have been reported recently [3–6]. However, the dielectric and piezoelectric properties of SBNT solid solution were presented only by Shimakawa et al. [7] and Sun et al. [8]. The aim of this paper is to present the results of detailed studies on crystal structure at room temperature, microstructure, dielectric properties and phase transition in chosen ceramic samples of SBN–SBT solid solution.

2. Experimental

The $SrBi_2(Nb_{1-x}Ta_x)_2O_9$ ceramics, (SBNT), with $x = 0.0$, 0.1, 0.2, 0.3, 0.5, 0.7 and 1.0 were prepared by a standard mixed-oxide method. Starting raw materials $SrCO_3$, Bi_2O_3, Ta_2O_5 and Nb_2O_5 (all from Aldrich), were weighted and mixed together for 24 h. The mixtures were pressed into pellets and then sintered for 2 h at 950 °C inside a closed double crucible. The obtained substances were crushed, milled in a ball mill and sieved. Such powders were pressed again into pellets and sintered for 2 h at 1150 °C.

The grain structure and distribution of all components throughout the grains were examined by a scanning electron microscope (SEM), JSM-5410, with an energy dispersion X-ray spectrometer (EDS) by Oxford Instruments. The metallographic specimens of all samples were analyzed as well. The crystal structure was analyzed by the X-ray diffraction (XRD,

* Corresponding author. Tel.: +48 32 3591134; fax: +48 32 2588431.
E-mail address: kajewski@us.edu.pl (D. Kajewski).

0272-8842/$34.00
doi:10.1016/j.ceramint.2009.01.013

STADI Diffractometer, Cu Kα radiation). The density of the investigated ceramics was determined by the Archimedes displacement method with distilled water. All the ceramic pellets were polished to obtain flat and parallel surfaces and were about 0.5 mm in thickness for dielectric measurements and for the observation of spontaneous polarization and the coercive field. The samples were coated with silver electrodes using a silver paste without thermal treatment and deaged at 500 °C for 10 min prior to measurements. The obtained ceramics were used for the measurements of the real part of permittivity (ε') and the dielectric loss (ε'') as a function of temperature and frequency of the measuring field. An automatic measuring system with HP 4192A impedance analyzer was used to measure and record ε' and ε''. The remnant polarization (P_r) was determined from the hysteresis loop measurements at room temperature in silicon oil. Hysteresis loops were measured using the RT6000HVS by Radiant Technologies.

3. Results and discussion

3.1. SEM and composition analysis

The observation of microstructure of $SrBi_2Nb_2O_9$ (SBN), $SrBi_2(Nb_{0.5}Ta_{0.5})_2O_9$ (SBNT 50/50) and $SrBi_2Ta_2O_9$ (SBT) ceramics was carried out. In all cases grains have plate-like shape with random orientation. This is one of the characteristics of bismuth layered structured ferroelectrics. The grain growth in these materials is much different than in isotropic ferroelectrics. The grain growth in *a*- and *b*-axis direction is much more forced than in the *c*-axis direction, which is perpendicular to the *a*–*b* plane. So the SBNT ceramics as one of BSLFs manifest a plate-like morphology. An addition of Ta leads to a decrease of the plate thickness from ∼2 μm for SBN to ∼1 μm for SBT. The metallographic analyses revealed that the angle between grain boundaries in SBN in most cases is around 120° and grains have rounded shape (Fig. 1a). The addition of Ta into SBN (Fig. 1b) causes the appearance of grains which predominate in the pure SBT (Fig. 1c).

Energy dispersion X-ray spectrometer (EDS) was used to check the distribution of individual elements within the grains.

Table 1
Concentration of elements from the EDS analysis.

Sample	Experimental (at.%)				Nominal (at.%)			
	Sr	Nb	Ta	Bi	Sr	Nb	Ta	Bi
SBN	19.14	38.97	–	41.89	20	40	–	40
SBNT 90/10	18.01	38.27	3.38	40.34	20	36	4	40
SBNT 80/20	17.77	35.04	6.86	40.32	20	32	8	40
SBNT 70/30	20.61	28.28	13.72	37.39	20	28	12	40
SBNT 50/50	22.39	15.91	23.87	37.83	20	20	20	40
SBNT 30/70	23.39	12.76	26.24	37.61	20	12	28	40
SBT	25.64	–	37.56	36.80	20	–	40	40

The EDS analysis indicated a homogeneous distribution of all elements of ceramics within the grains. Moreover, the quantitative microanalysis performed with the implementation of SEMQuant programs elaborated by Oxford Instruments showed that all samples had the stoichiometry close to nominal (Table 1).

3.2. XRD analysis and density

The calculations were performed using the software for treatment of powder X-ray diffraction data DHN_PDS. In order to receive exact locations, intensities and widths of diffraction lines, the experimental data were fitted to theoretical functions. The attempts at fitting by Gaussian (G), Lorenzian (L), modified Lorenzian (ML) and intermediate Lorenzian (IL) were made. The IL profile showed the best agreement with experimental data and this profile was used to fit all segments of the diagram including the diffraction lines.

The XRD patterns of SBNT ceramics obtained at room temperature are shown in Fig. 2. They exhibit an Aurivillius structure but no other phase is observed. We have confirmed the structure of our SBNT ceramics by fully indexing the observed peaks of the XRD spectrum according to $A2_1am$ symmetry. The strongest diffraction peak for all SBNT samples is (1 1 5), which is consistent with the (112*m*+1) highest diffraction peak in Aurivillius phase [9]. It is noticeable that the intensity of the (0 0 4) diffraction peak decreases gradually with the increase of Ta content. The *a* and *b* lattice constants are equal to each other within the error (±0.002 Å). There are no changes of these

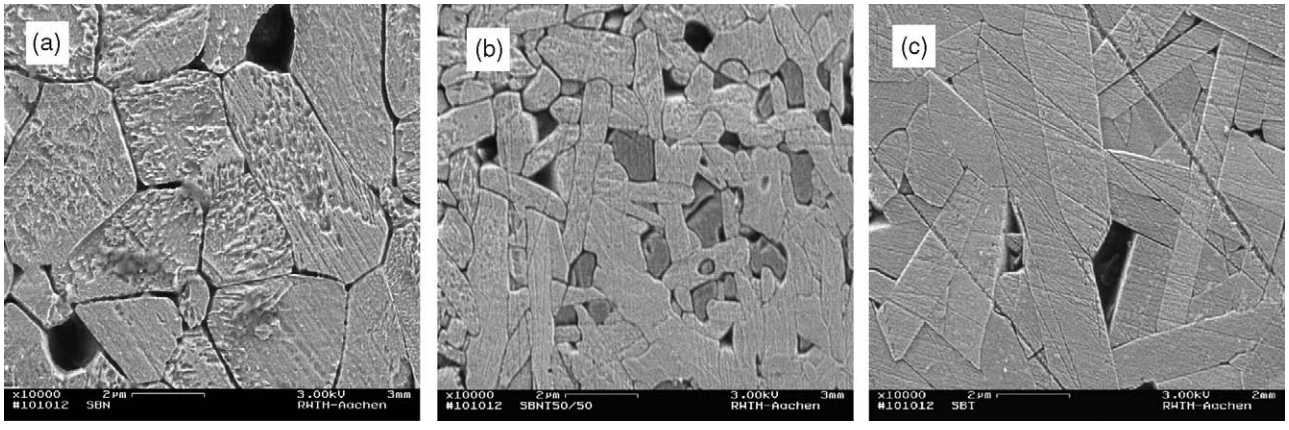

Fig. 1. SEM images of the surface after metallographic specimen of SBN (a), SBNT 50/50 (b) and SBT (c).

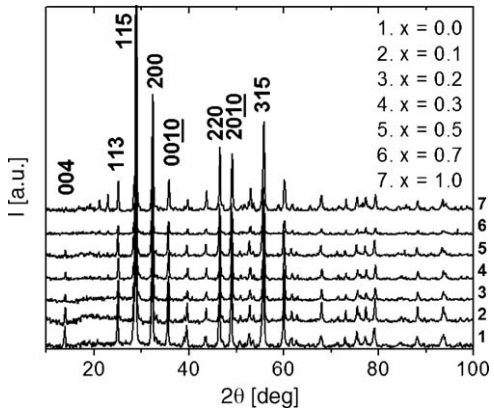

Fig. 2. Part of the diffraction patterns obtained at the room temperature of the $SrBi_2(Nb_{1-x}Ta_x)_2O_9$ ceramics.

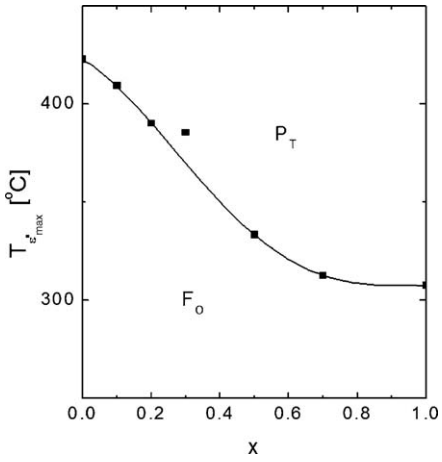

Fig. 4. Variations of phase transition temperature vs. Ta content.

constants with the changes of SBT content in SBN and their values are about 5.497 Å. The *c* lattice constant decreases from 25.10 to 24.94 Å linearly with increasing amount of Ta in the solid solution. Obtained results are in very good agreement with previous investigations [10,11].

The calculations of the density were performed for a comparison with results obtained by the Archimedes method. The experimental density is about 93% of the theoretical one calculated from the XRD measurements. Such a difference is caused mainly by pores. The density increases linearly with the increase of Ta content from about 6.7 g/cm^3 (experimental), 7.25 g/cm^3 (theoretical) to 8.2 g/cm^3 (experimental), 8.75 g/cm^3 (theoretical) for SBN and SBT, respectively.

3.3. Dielectric properties and investigations of hysteresis loops

The samples were treated as plate capacitors and it was possible to calculate the real part of permittivity (ε') and dielectric loses (ε''). The comparison of ε'(T) and ε''(T) plots for SBNT ceramics is shown in Fig. 3a and b, respectively. The characteristics were obtained at the measuring field of 100 kHz frequency. In the low temperature range, ε' is around 100 for all samples and exhibits small changes with temperature. Moreover ε'' values are small in the temperature range from about 200 °C down to room temperature. Both ε'(T) and ε''(T) reveal anomalies associated with phase transition from the tetragonal paraelectric phase (P_T) to the orthorhombic ferroelectric phase (F_O). One can see that the position of anomalies in ε'(T) and ε''(T) plots, corresponding to P_T–F_O phase transition, are strongly dependent on the Ta content. The changes of the temperature T_M at which the anomalies in ε'(T) appear, with the changes of the content of the ceramics are shown in Fig. 4. Both the real part of permittivity peak and dielectric loss peak shift gradually towards lower temperatures as the Ta content (x) increases.

The presented plots of ε'(T) show a diffuse character of the P_T–F_O phase transition causing the observed deviations from the Curie–Weiss law in the range of the paraelectric phase up to T_B temperature which can be interpreted as Burns' temperature

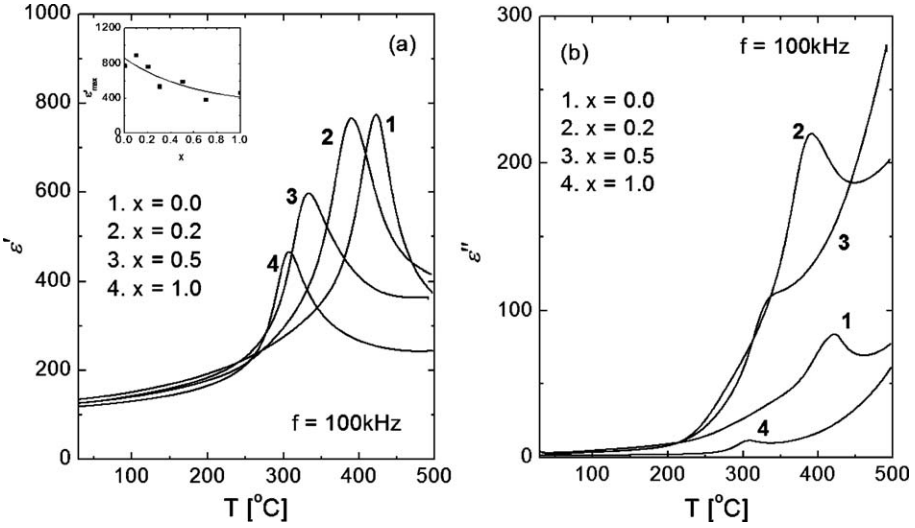

Fig. 3. Real part of permittivity vs. temperature (a), dielectric losses vs. temperature (b) in $SrBi_2(Nb_{1-x}Ta_x)_2O_9$ ceramics and variations of the maximum of the real part of permittivity vs. Ta content (inset).

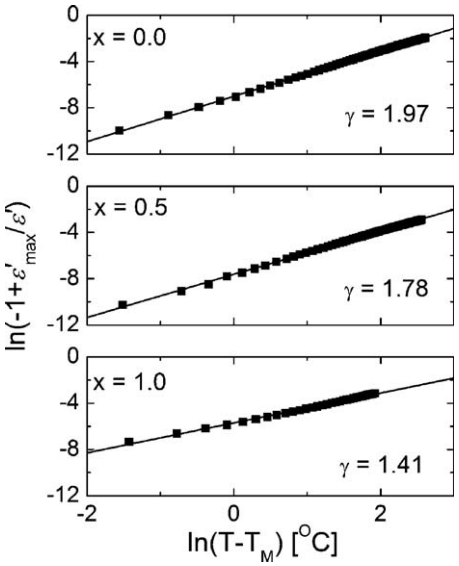

Fig. 5. $\ln(-1+\varepsilon'_{max}/\varepsilon')$ vs. $\ln(T-T_M)$ at 100 kHz in the temperature range between T_M and T_B for $SrBi_2(Nb_{1-x}Ta_x)_2O_9$ ceramics.

[12,13]. The attempt to test the Curie–Weiss law above T_B was made for all samples. It was successful only in the narrow range of temperatures in all samples except SBNT 30/70. The Curie constant (C) value is oscillating around 0.8×10^5 °C. The gradual decrease of the Curie–Weiss temperature (T_0) from 395 to 224 °C was observed for SBN with enhancing amount of Ta.

The quantitative assessment of the diffusion (γ) in the paraelectric phase in the temperature range between T_M and T_B, was evaluated by the expression [14]

$$\frac{1}{\varepsilon'} - \frac{1}{\varepsilon'_{max}} = \frac{(T-T_M)^\gamma}{C'} \quad (1)$$

where γ and C' are constants. The exemplary plots are shown in Fig. 5. It is known that the value of γ ($1 \le \gamma \le 2$) is the expression of the degree of diffusion of the phase transition.

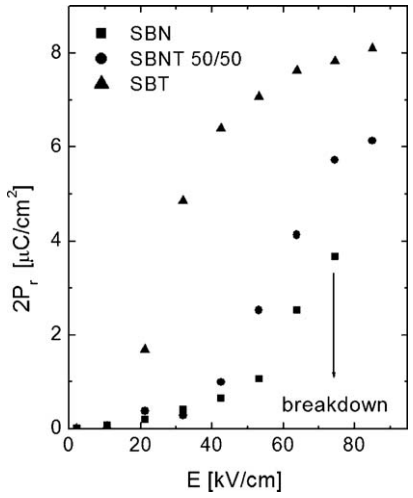

Fig. 7. Remnant polarization vs. intensity of measuring field for chosen $SrBi_2(Nb_{1-x}Ta_x)_2O_9$ ceramics.

The γ value increases from 1.41 to 1.97, for SBT and SBN ceramics, respectively. This may suggest that the diffuseness of the phase transition is caused not only by the fluctuation of chemical composition but also by inner electric fields and tensions which are the results of creation of vacancies.

The measurements of ε'(T) at various frequencies of the measuring field, were performed to check the existence of relaxor properties of the samples. The exemplary curves are shown in Fig. 6. The ε'(T) characteristics show a decrease of the ε' value at the temperature higher than 150 °C with an increase of the measuring field frequency, and an intensification of the low frequency dispersion in the ferroelectric phase. The dispersion may occur due to the Sr/Bi cation exchange [15,16] during synthesis process and from the volatilization of Bi_2O_3 at high temperatures leading to the creation of oxygen vacancies [17]. That leads to induced polarization which becomes dominant at high temperatures and low frequencies.

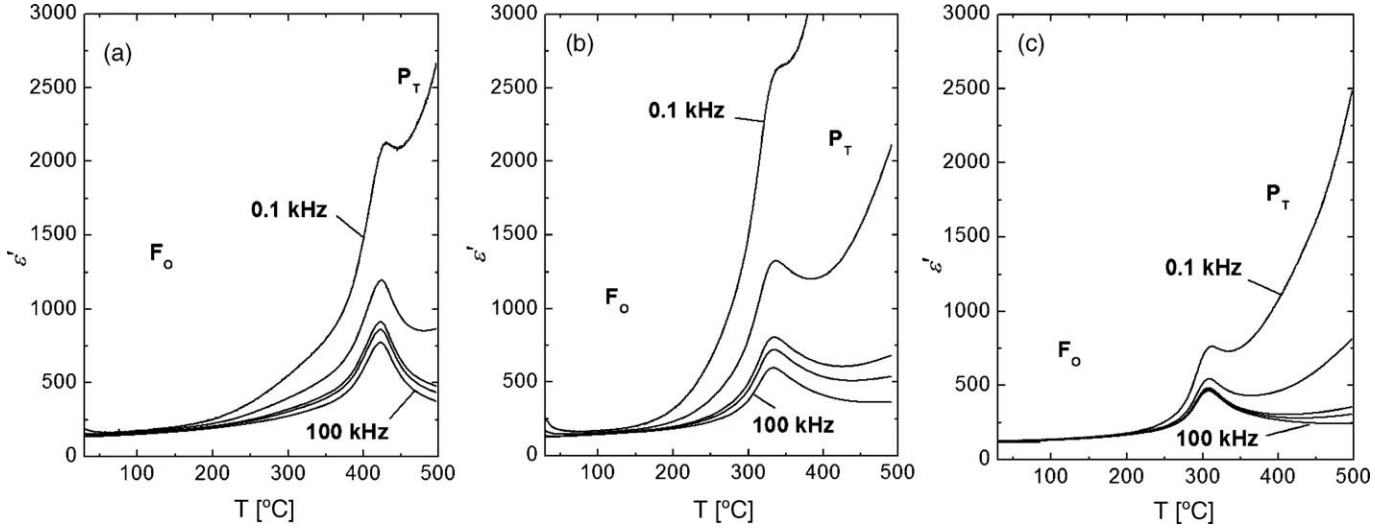

Fig. 6. Real part of permittivity as a function of temperature measured on cooling at various frequencies of measuring field, for SBN (a), SBNT 50/50 (b) and SBT (c) ceramics. The individual curves plotted for the frequency: 0.1; 1; 10; 20 and 100 kHz.

All ε'(T) plots exhibit no shift of the temperature T_M with frequency. Such a shift is typical for ferroelectric relaxors [18]. Moreover, an additional increase of the ε'(T) curves were observed in the range of higher temperatures in the paraelectric phase which point to the low frequency dispersion in all samples. Such dispersion has also been reported by others [19].

The investigation of P–E hysteresis loops for SBN, SBNT 50/50 and SBT ceramics was performed also. The measurements were made at the room temperature and under driving field from 2 to 85 kV/cm in the virtual ground mode. Only the hysteresis loop for the SBT sample has approached saturation. All observed loops were shifted into negative field values which could be caused by existence of oxygen vacancies. Such phenomenon was also observed for SBNT thin-film capacitors [20]. From performed measurements it was possible to determine relationship between remnant polarization of the samples and intensity of measuring field. The dependence is shown in Fig. 7. Remnant polarization in SBT sample is much smaller than reported by Shimakawa et al. [7]. Authors of the publication [7] have calculated the polarization from the atoms displacement using the simple ionic model which does not take into account the anisotropy of ceramics, screening process and existence of amorphous phase in ceramics. Those could be reasons of differences in mentioned value of polarization.

4. Conclusions

The results obtained for SBN–SBT solid solution can be summarized as follows.

(1) We were able to obtain the solid solution SBN–SBT with $A2_1am$ symmetry at room temperature, where the a and b lattice constants do not change with the increase of Ta content. However, the c lattice constant decrease with the increasing amount of Ta.
(2) It was possible to determine the temperature of the phase transition (T_M) from the paraelectric to the ferroelectric state from ε'(T) measurements. The T_M temperature decrease from ~420 °C for SBN to ~310 °C for SBT.
(3) The phase transition exhibits diffuse character and the strong low frequency dispersion however; the solid solution does not exhibit relaxor behavior such as $BaBi_2Nb_2O_9$–$BaBi_2Ta_2O_9$ solid solution. The reason of the dispersion may lie in the tendency to creation of defects in the crystal lattice especially in Bi, Sr and O sublattices.
(4) The lack of relaxor behavior in SBN–SBT solid solution may lie in smaller cation disorder in Sr/Bi sublattice than in Ba/Bi sublattice in $BaBi_2Nb_2O_9$–$BaBi_2Ta_2O_9$ solid solution what was reported for SBN and SBT samples by Nuzhnyy et al. [21].
(5) The problem of Sr/Bi cation disorder in SBN–SBT system is not clear yet and should be carefully studied since it could be a reason of dispersion of dielectric response.

Acknowledgements

Authors are very grateful to Miss Gisela Wasse from Institut für Werkstoffe der Elektrotechnik II RWTH Aachen for preparing the metallographic specimen.

References

[1] C. A-Paz de Araujo, J.D. Cuchlaro, L.D. McMillan, M.C. Scott, J.F. Scott, Fatigue-free ferroelectric capacitors with platinum electrodes, Nature 374 (1995) 627–629.
[2] B. Aurivillius, P.H. Fang, Ferroelectricity in the compound $Ba_2Bi_4Ti_5O_{18}$, Phys. Rev. 126 (1962) 893–896.
[3] B. Jimenez, P. Duran-Martin, A. Castro, P. Millan, Obtention and characterization of modified $Bi_2SrNb_2O_9$ Aurivillius-type ceramics, Ferroelectrics 186 (1996) 93–96.
[4] P. Duran-Martin, A. Castro, P. Millan, B. Jimenez, Influence of Bi-site substitution on the ferroelectricity of the Aurivillius compound $Bi_2SrNb_2O_9$, J. Mater. Res. 13 (1998) 2565–2579.
[5] Y. Wu, G. Cao, Enhanced ferroelectric properties and lowered processing temperatures of strontium bismuth niobiates with vanadium doping, Appl. Phys. Lett. 75 (1999) 2650–2655.
[6] P. Millan, A. Ramirez, A. Castro, Substitution of smaller Sb^{3+} and Sn^{2+} cations for Bi^{3+} in Aurivillius-like phases, J. Mater. Sci. Lett. 14 (1995) 1657–1660.
[7] Y. Shimakawa, Y. Kubo, Y. Tauchi, T. Kamiyama, H. Asano, F. Izumi, Appl. Phys. Lett. 77 (2000) 2749–2751.
[8] L. Sun, Ch. Feng, L. Chen, S. Huang, X. Wen, Piezoelectric and ferroelectric properties of $SrBi_2(Nb_{1-x}Ta_x)_2O_9$ ceramics, Mater. Sci. Eng. B 135 (2006) 60–64.
[9] X.F. Du, I.W. Chen, Ferroelectric thin film of bismuth-containing layered perovskites: Part I, $Bi_4Ti_3O_{12}$, J. Am. Ceram. Soc. 81 (1998) 3253–3259.
[10] Ismunandar, B.J. Kennedy, Gunawan, Marsongkohadi, Structure of $ABi_2Nb_2O_9$ (A = Sr, Ba): refinement of powder neutron diffraction data, J. Solid State Chem. 126 (1996) 135–141.
[11] A.D. Rae, J.G. Thompson, R.L. Withers, Structure refinement of commensurately modulated bismuth strontium tantalite, $Bi_2SrTa_2O_9$, Acta Cryst. B: Struct. Sci. 48 (1992) 418–428.
[12] G. Burns, F.H. Dacol, Polarization in the cubic phase of $BaTiO_3$, Solid State Commun. 42 (1982) 9–12.
[13] G. Burns, F.H. Dacol, Ferroelectrics with a glassy polarization phase, Ferroelectrics 104 (1990) 25–35.
[14] H.T. Martinera, J.C. Burfoot, Grain-size effects on properties of some ferroelectric ceramics, J. Phys. C: Solid State Phys. 7 (1974) 3182–3192.
[15] A.C. Palanduz, D.M. Smyth, Defect chemistry and charge transport in $SrBi_2Nb_2O_9$, J. Electroceram. 11 (2003) 191–206.
[16] A.C. Palanduz, D.M. Smyth, Defect chemistry of $SrBi_2Ta_2O_9$ and ferroelectric fatigue endurance, J. Electroceram. 5 (2000) 21–30.
[17] B.H. Park, S.J. Hyun, S.D. Bu, T.W. Noh, J. Lee, H.-D. Kim, Differences in nature of defects between $SrBi_2Ta_2O_9$ and $Bi_4Ti_3O_{12}$, Appl. Phys. Lett. 74 (1999) 1907–1909.
[18] Z.Y. Cheng, R.S. Katiyar, X. Yao, A.S. Bhalla, Temperature dependence of the dielectric constant of relaxor ferroelectrics, Phys. Rev. B 57 (1998) 8166–8177.
[19] I. Coondoo, A.K. Jha, S.K. Agarwal, Enhancement of dielectric characteristics in donor doped Aurivillius $SrBi_2Ta_2O_9$ ferroelectric ceramics, J. Eur. Ceram. Soc. 27 (2007) 253–260.
[20] A. Furuya, J.D. Cuchiaro, Composition dependence of electrical characteristics of $SrBi_2(Ta_{1-x}Nb_x)_2O_9$ thin-film capacitors, J. Appl. Phys. 84 (1998) 6788–6794.
[21] D. Nuzhnyy, S. Kamba, P. Kužel, S. Veljko, V. Bovtun, M. Savinov, J. Petzelt, H. Amorín, M.E.V. Costa, A.L. Kholkin, Ph. Boullay, M. Adamczyk, Dynamics of the phase transitions in Bi-layered ferroelectrics with Aurivillius structure: dielectric response in the terahertz spectral range, Phys. Rev. B 74 (2006) 134105.